HIGH FIELD Q DROP IN SUPERCONDUCTING GHz CAVITIES

J. Halbritter, Bau 421, Postfach 3640, 76021 Karlsruhe, Germany.

Abstract

In rf cavities dielectric surface losses R^E are usually neglected as compared to magnetic rf losses R^B where the latter become very small well below the superconducting critical temperature T_c. But the high density of localized states $n_L(z_L)>10^{21}/cm^3$ of Nb_2O_5 adjacent to the high conduction electron density $n_C=6\cdot10^{22}/cm^3$ of Nb yield measurable dielectric surface impedances Z_{ITE} by strong *interface tunnel exchange (ITE) between $n_L(z_L)$ and n_C* . For E>1MV/m the energy gain $ez_LE(t)$ lifts $n_L(z_L,\varepsilon<-\Delta)$- up to $n_L(z_L,\varepsilon>\Delta)$- states ITE coupled to empty $n_C(\varepsilon>\Delta)$ states. Only some of those broken pairs are able to escape into delocalized regions $n_C(\varepsilon>\Delta_{ave})$ creating hot excitations being BCS amplified dominating the rf absorption as exponential, field emission free, high *field Q drop (HFQ)* above 10 – 30 MV/m.

INTRODUCTION

Metal - dielectric interfaces influence the dc and rf conduction of metals by the intimate contact of extended conduction electron states $n_C(z_L)$ with localized states $n_L(z_L\geq0,\varepsilon)$ in the rf surface impedances Z = R + iX, i.e. surface resistance R and penetration depth $\lambda=X/\omega\mu_0$ [1-8]. Because of the strong Nb - O bonds and after standard treatment, i.e. 100 -200µm Nb damage layer removal by electro polishing (EP) or buffered chemical polishing (BCP) high pressure (80 bar) water rinsing (HPR) is applied [1,7]. HPR removes about 10 nm followed by wet oxidation serrating interfaces as sketched in Fig. 1 [5-8] and summarized below: starting from the vacuum side, by its strong hydrogen bonds the NbOOH surface is coated by *2 – 10 monolayers (ML) of H_2O and hydro-carbons* [10-11a], where 2 ML cannot be removed by UHV annealing below about 300°C. NbOOH terminates *≥4nm Nb_2O_5* connecting to about 0.5nm metallic $NbO_x(x\leq1)$ and Nb containing O in solid solution and Nb_2O_5, NbO_x, and NbO_6 precipitates. Depending on Nb treatment after oxidation Nb_2O_5, NbO_x, and NbO_6 precipitates are found in Nb up to 100µm deep.

Using [3] the surface impedance Z^E by interface tunnel exchange (ITE) between $n_C(\varepsilon)$ and $n_L(z_L,\varepsilon)$ is worked out in [5] and compared to experiments here shortly. Superconducting Nb GHz accelerator cavities are limited by this field emission free, high field Q drop (HFQ) at peak field E_p above 30 to 70 MeV/m and $B_p\geq0.08$ –0.18T [1,8]. According to [5] HFQ is based on rf fields >1MV/m in Nb_2O_5 acting on $n_L(z>1nm)$ states yielding an energy gain $2ezE>3.1meV=2\Delta(Nb)$ in half a rf period causing the exponentially increasing as HFQ *source term $b_s s(E)$*. Some of those ITE broken pairs $\varepsilon^*>\Delta_{ave}$ escape from the interface and decay into hot excitations in an

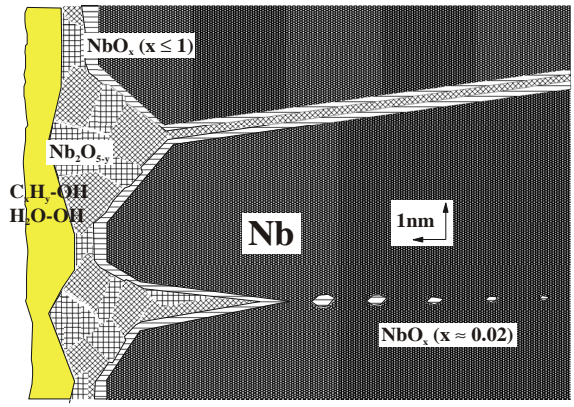

Figure 1: Nb surface with crack corrosion by wet oxidation by Nb_2O_5 volume expansion (factor 3). Nb_2O_{5-y}-NbO_x weak links/segregates (y, x < 1) extend up to depths between 0.1 – 1/ 1-100 µm for good – bad Nb quality and weak - strong oxidation [8-11]. The adsorbate layer being chemisorbed by hydrogen bonds to $NbO_x(OH)_y$ H_2O/C_xH_yOH (≥3nm) may contain, e.g. dust

area $A_{ITE}(E)$ as *HFQ valve term*, which get BCS amplified causing the *HFQ loss term $B^2bs(E)$*. The BCS rf quanta are transferred ballistically to, e.g. the outer He/Nb interface, yielding hot spots $\Delta T_{ou}(E)$ proportional to $R_{HFQ}(E)$ increasing exponentially with E. The ITE theory combined with Nb_2O_5 material parameters and HFQ results are fitted quantitatively with one free fit parameter b in Sect.4.

OXIDATION OF Nb

The b(Nb-O) binding energies of 7eV in Nb-O chemisorptions layers and of 5eV in bulk Nb_2O_5 are in excess of b(Nb-Nb) = 1.9 and b(O-O) =2.5eV yielding strong solution of O inside Nb and fast chemisorption of O at Nb surfaces in air [8-10]. As *first step in oxidation,* O dissolves atomically in the open Nb lattice and migrates along grain boundaries and dislocations into the interior. O may precipitate as metallic Nb_6O or $NbO_x(x\leq1)$ spots or layers and as dielectric, nano crystalline Nb_2O_5 if the volume expansion by O-Nb d-bonding is taken care off. Below about 500K as a *second oxidation step* the *Cabrera Mott growth of Nb_2O_5* based on the binding energy potential $V^O{}_m\approx0.6V=b(O\text{-}O)-b(Nb\text{-}Nb)$ causes NbO_x electrons $n_C(E_F)$ to tunnel through the Nb_2O_5 coating charging chemisorbed O_2 from lab air or vacuum. This yields electrochemical like growth where $V^O{}_m$ drives mainly O ions through Nb_2O_5 toward the metallic $NbO_x(x\leq1)$ surface to be discharged there forming either Nb_2O_{5-y} with a factor three larger volume or being injected into Nb. Nb_2O_{5-y} consists of edge connected NbO octahedra blocks (CB) corres-ponding to valence 6, which in turn get side connected via crystallographic shear

planes (CS) housing oxygen vacancies V_O to achieve the proper valence 5 [8]. Separated by CSs then nano crystalline CBs nucleate depending on the detailed morphology of the metallic NbO_x/ Nb_6O/Nb interface. The strain onto the soft Nb is relaxed by creation of dislocations which promote the O diffusion deep into the Nb, like along grain boundaries, causing crack corrosion sketched in Fig.1. In wet oxidation CSs enforce Cabrera Mott growth by high n_L- den-sities and low barrier heights Φ_S=0.1eV [9] speeding up e^- tunnelling and V_Os enforcing the O migration via place exchanges [10] and causing dislocations relaxing strain. In contrast, in dry oxidation Cabrera Mott growth is retarded by CBs by their high tunnel barrier Φ_B=0.6eV and low n_L-densities.

HFQ SOURCE TERM

In rf cavities the dielectric surface impedance Z^E(E<1MV/m) of Nb_2O_5 coatings is usually negligible [6a]. But high densities $n_L(z_L)\leq 10^{21}/cm^3$ and low Φ_S=0.1eV of Nb_2O_5 enforce ITE. Quantitatively, ITE [3] is given by the tunnel rate between n_C and exponentially decaying wave functions inside the oxide. The occupation $n_C(\varepsilon)$ follows the Fermi distribution function $f(\varepsilon)=1/\{1+\exp(E-E_F)/kT\}$ and the occupation $n(z_L,\varepsilon_L,t)$ of $n_L(z_L,\varepsilon_L)$ changes with applied electric field $\Delta\varepsilon$ = ezE(t) being repopulated with the rate $1/\tau(z,\varepsilon)=1/\tau(0,\varepsilon)\exp(-2z\kappa)g(z\kappa)$. $\omega\tau(z^*,\varepsilon)=1=\omega\tau(0,\varepsilon)\exp(-2z^*\kappa)$ defines the *fast exchange distance* z^* up to which $f(\varepsilon)n_L(\varepsilon,z\leq z^*)$ is in equilibrium with $f(\varepsilon)n_C$ [3]. In scs by opening of the BCS energy gap the density of state $n_C(\varepsilon\approx E_F)$ becomes energy dependent $n_C(\varepsilon^*)= n_C(E_F)\ |\varepsilon^*|/\sqrt{\varepsilon^{*2}-\Delta^2}$. ITE pair breaking is due to tunnelling from occupied states $n_c(\varepsilon^*\leq-\Delta)$ around $\omega t \approx(2n+1)\pi$ (n=0,1,2….) of E(t) = E(0)cos(ωt) into empty trap states $n_L(z,\varepsilon^*_0)$ below -Δ. with $\varepsilon^* =\varepsilon^*_0-ezE(t)$. Those states gain energy $\Delta\varepsilon_0=2ezE(t)$ in half an rf period $\pi/2 \leq\omega t \leq+ \pi3/2$ able to tunnel back around $\omega t \approx(2n)\pi$ (n=0,1,2..) for $\Delta\varepsilon_0\geq 2\Delta$ and for $\varepsilon^*_0+ezE(t)\geq\Delta$ into empty $n_C(\varepsilon^*)$ states of the superconductor. With $x^* =\min\{z^*,d_O\}$, pair breaking onset distance $x^*=\Delta/eE^0$, onset field E^0, $c=2\kappa\Delta/e$ and $\beta^*=1$ this is approximated by

$$P_{ITE}=\{f\pi n_L/2\tau(0)\}(2eE)^2/(2\kappa)^3\{2[\exp(-c/E)-\exp(c/E^0)]+2[\exp(-c/E)c/E-\exp(-c/E^0)c/E^0]+[\exp(-c/E)(c/E^\perp)^2-\exp(c/E^0)(c/E^0)^2]\}=f\pi n_L/2\tau(0)(2eE)^2/(2\kappa)^3 s(-c/E^\perp,c/E^0)=\varepsilon_0/2\mu_0 R_{ITE}{}^E E^2 \quad (2.1)$$

For Nb_2O_{5-y} P_{ITE} is dominated by CSs with Φ_S=0.1eV, i.e. κ_S = 1.6/nm, yielding $c_S = 2\kappa\Delta\ \varepsilon_r/e\beta^*$= 130 - 400 MV/m by Δ = 1.5 meV and by ε_{rS} = 20 increasing up to about ε_{rS} = 60 with n_L where $n^S_L\approx 10^{20}/eVcm^3$ is typical for wet oxidized Nb [8].

MAGNETIC RF LOSSES AND OXIDATION OF NB

The superconductivity of clean, metallic, Nb with T_c = 9.25K and Δ_0/kT_c = 2.05 degrades by oxidation where O in solid solution reduces T_c and Δ by 10% for 1 at% O.

$R_{BCS}(T,\omega) = r_0\omega^\beta\exp(-\Delta/kT)/kT;\quad T \leq T_c/2,\ \hbar\omega\leq\Delta/30$ (3.1) fits oxidized bulk Nb- and Nb film- rf cavities excellently with agreement experiment/theory above 6 orders magnitude [1,2,8]. For typical oxidized Nb surfaces $\Delta\leq$1.5meV, Δ/kT_c=1.7-1.9 and β=2 are obtained describing properties averaged over the penetration layer ≈100nm. States $n_L(\varepsilon,z\geq$0.3nm) are normal conducting by pair weakening [9b] causing rf residual losses by Nb_2O_5 filled weak links (WL) $R^{WL}_{res}(T,\omega) \geq 1n\Omega(f/GHz)^2$ [7b,c]. Above ac/rf field amplitudes B_{c1J}/B_{c1} and frequencies below $\omega_o{}^J/\omega_o{}^A$ hysteresis losses by Josephson fluxons (JF) R_{hys} =4/3π·λ_{hys}= R^1B/B_c occur by JFs $\omega_0{}^J\leq 10^{10}$Hz as compared to slow $\omega_0{}^A\approx$MHz of Abrikosov fluxons (AF). O pick-up not only yields Nb_2O_5- but also Nb_6O- or NbO_x- precipitates, i.e. regions with $\Delta^*<\Delta_0$. Such locally confined quasiparticles $|\varepsilon|\leq\Delta_{ave}$ are easily driven out of thermal equilibrium yielding the low field Q-slope (LFQ) $R_s(T,<40\ mT) = a(T)/B^2 + R_{BCS}(T,\sim 10mT) + R_{res}$. The accompanied gap smearing reduces R_{BCS} with ß(<10GHz)= 2. Nb_6O or NbO_x precipitates or O in solid solution show up in $Z(H_{dc},<$MHz) impedances [12] by deteriorated critical fields H_{c1}, H_{c2}, or H_{c3} and by pinning of AFs. In summary:

- *wet oxidation at 300K* yields plenty of CSs corresponding to plenty dislocations promoting strong O, NbO_6 and Nb_2O_5 injection into Nb having been observed as up to 10 at% O in the first 10nm [11a], as $\Delta/kT_c(10mT)\approx$1.75 for cold worked, RRR~40 Nb [8] or large grain Nb [15c], as degradation of H_{c1}, H_{c2}, or H_{c3} and as pinning [8,12]. The pinning by cold working reaches depth of 50 – 100µm and by oxidation depth of 5µm [12]. In small grained or RRR~40 Nb O precipitates at defects reducing R_{BCS}(T, <15GHz) with Δ/kT_c(>5mT)≈1.85 and strong LFQ [7b];
- *dry oxidation* creates less dislocations in Nb transferring O into depth of about 5µm for RRR~40, as found by pinning where the accompanied degradation of H_{c1}, H_{c2}, or H_{c3} has been found for RRR~200 Nb also [12] and Δ/kT_c degrades from 1.9 to 1.85 for RRR~40 Nb [8].
- *UHV or air baking around 120°C* of wet oxidized Nb reduces the dislocation density [11b] but $\Delta^*<\Delta_{ave}$ cluster grow in density and extension shown by decreasing R_{BCS}(T,<15GHz), by enforced LFQ [15a], by weakened WLs, i.e. R^{WL}_{res}, R_{hys} and MFQ grow.

HEAT TRANSFER IN SUPERCONDUCTING NB

Rf dissipation heats the inner surface by ΔT_{in} as compared to the He bath T_0 usually described by heat diffusion. The exponential growth of $R^B_{BCS}(T)$ with ΔT_{in} yields the medium field Q slope MFQ $\gamma^*(T)(B/0.2T)^2$. Heat diffusion assumes that all mean free paths, i.e. of phonons l_{ph} and (inelastic) electrons l_{in} are very short compared to lengths involved [13]. But in sc's the pair condensation reduces exchanges between quasiparticles, between phonons and between quasiparticles and phonons, enhancing mean free paths drastically. R_{BCS} rf photons excite quasiparticles, which transfer the gained energy

$\hbar\omega<\Delta/30$ to phonons $l_{in}=v_F\tau_{in}(T,<10GHz)>6\cdot10^{-3}(T_c/T)^3$cm, being similar long as for phonons $l_{ph}(\leq 2K,4GHz)\geq 1$cm. Hence, $|\varepsilon|\leq\Delta_{ave}$ broken ITE pairs stay localized and thermalize to phonons slowly [5]. But some *delocalised ITE broken pairs* sneak into regions with extended states $|\varepsilon|\geq\Delta_{ave}$ and decay with $l_{in}(>\Delta)\geq 10\mu$m [13] *in a seam along the surface larger than* $\pi(10\mu m)^2=A^0_{ITE}=10^{-7}cm^2$. Those hot quasiparticles $f^*(\varepsilon^*\geq\Delta_{ave})$ may radiate and decay further to the gap edge yielding $f^*(\varepsilon^*\geq\Delta_{ave})$ over rapidly expanding regions A^*_{ITE} growing with E acting as *HFQ valve term.* Hot quasiparticles $f^*(\varepsilon^*\geq\Delta_{ave})$ described by $T+\Delta T^*_{in}=T_c$ causes $R_{BCS}(2K+\Delta T^*_{in})$ enhancements up to 8 orders of magnitude at GHz as compared to $R_{BCS}(2K)$ [2b]. As HFQ loss term the so excited BCS quasiparticles radiate ballistically yielding

$$\Delta T_{ou}(E,\mathbf{r}) = B^2 b_T s(-c/E^{\perp},-c/E^0) \propto \delta f^*(\varepsilon^*,\mathbf{r}^*)\propto R^E(E,\mathbf{r}) \quad (4.2)$$

adding up to

$$R^{HFQ}(E)=b_A B^2/E^2 s(-c/E^{\perp},-c/E^0)+R^E_S \text{ with } b_A\propto A^{**}_{ITE} \quad (4.3)$$

Rf losses, like R^{WL}_{res} and R_{hys}, *thermalize locally* at WLs with large ΔT_0 values [7c] by the standard heat diffusion. In contrast ballistic processes, e.g. by $R_{BCS}(T)$ or by HFQ, do not yield thermal runaway but a fast and large lateral spread A^{**}_{ITE} promoted by the homogeneity of the inner surface shown, e.g. in Fig.2. Remarkable is the fact that a nano roughness $ß_{ave}$ averaged over $A_{ITE}>10^{-7}cm^2$ defines local onset fields $ß_{ave}E_{loc}/\varepsilon_r(d,n_L)>1.5$MV/m above which broken ITE pairs are B^2R_{BCS} amplified which finally cause the HFQ loss term $B^2b_s(-c/E^{\perp},-c/E^0)$.

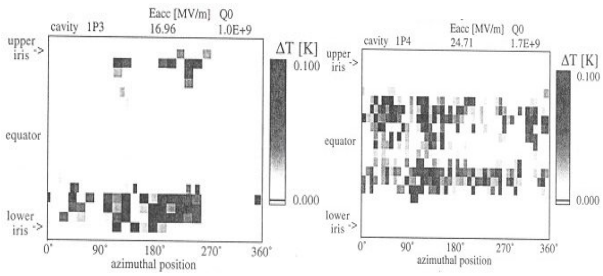

Figure 2: Heat maps for spun Nb cavities (1.3GHz, Bp/Ep =2.1mT/MV/m, Eacc= EP/1.78) of reactor grade Nb (RRR ≈30) at fields just below the quench at Bcrit with HFQ increases shown in Fig. 5 [14]. The maximum temperature rise was 0.4K. By BCP smoothening the rotational symmetric heating shifts away from the iris.

EXPERIMENTAL RESULTS ON $R^E(T,E)$

Above about 10MeV/m accelerating field $E_{acc}=E_P/1.78$ HFQ has been found in Nb TM cavities (B_P/E_P= 2.5mT/MV/m) being discussed in [4,7,14,15] already. As shown in Fig.2 [14], HFQ hot spots are organized on rings $E_{loc}(r)$ = const moving toward the equator with enforced BCP stripping. The heat maps and the corresponding field dependencies R(E,B) after 50, 120 (P3), 130 and 230 µm (P4) BCP stripping show HFQ improvements fitting to Eq.(2.1) excellently in Figs.3. The fit fields c and E^0 of rough, cold worked spun RRR>250 Nb in Table 1 increase from c=100 to 470MV/m and the hot spot position move toward the equator from E_p to $E_p/5$ and B_{max}=70 to 100 mT for 230µm BCP. Results of a small grained (~ 50µm), smooth, RRR > 300, air baked Nb cavity show exponential R(E) and of $\Delta T_{ou}(B,r)$ increases in Figs.4 and 5 fitted to Eq.(2.1) in Tables 2, 3 and [15a,b] and hot spots starting at least 2cm away from the equator expanding with further increasing rf field toward the

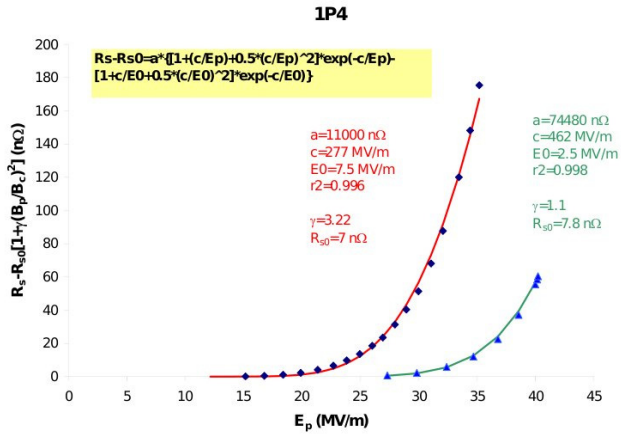

Figure 3: RHFQ(2K,Eacc) of spun, i.e. coldworked, Nb TM010-mode cavities at 1.3GHz of RRR ~250 Nb sheath [14] after 120µm BCP for P3 and 230/290 µm for P4 with HFQ fit parameters summarized in Table 1. ßave<4 is reduced by smoothening and higher BP fields are reached so that MFQ has to be subtracted.

Table 1: Fitted ITE fields to Eq.(2.1) of seamless, single cell, 1.3GHz TM_{010}, heavily coldworked, i.e. spun Nb rf cavities measured at 2K with results shown in Figs. 2 and 3 [14]. After subtracting $a(2K)/B^2$ (LFQ), R_{res} and MFQ, ITE fits where performed. The average roughness and damage caused by spinning was reduced by successive BCP stripping between 50 and 230µm shifting hot spot positions from E_p to $E_p/5$ and enhancing B_{Pmax} from 40 to 100mT. ITE fit fields c_P and E^0_P have to be corrected to c_{loc}=100-200MV/m and E^0_{loc}~1-2MV/m.

BCP/ µm	R_{res}/ nΩ	a/µΩ/ $(mT)^2$	γ^*	b/ µΩ	c_P/ MV/m	E_P^0/ MV/m	E_{loc}/E_p
50	~5	-	-	5	100	1	-
120	7.5	8.9	-	7	204	8	<1
130	7.8	8.7	1.1	10	275	9	-
230	7	-	3.2	74	462	2.5	~1/5

equator. This expansion and the exponentially with field increasing $\Delta T_{ou}(B)$ values cannot be explained by local thermal equilibrium and standard heat diffusion originating at loss spots, as elucidated in [15a]. The results of bulk, small grained, RRR > 200 Nb cavities after repeated BCP followed by wet oxidation, anodization and baking [15a,b] fitted to Eq.(2.1) show that

baking does not change c and E^0 markedly, whereas the b values of Eq.(4.3) changes by 2 to 3 orders of magnitude.

As summarized in Table 2 and in [14,15] baking enhan-ces R_{res}, LFQ of, Δ/kT_c, R^1 and γ^*, whereas $R_{BCS}(T,f< 15GHz)$ decreases.

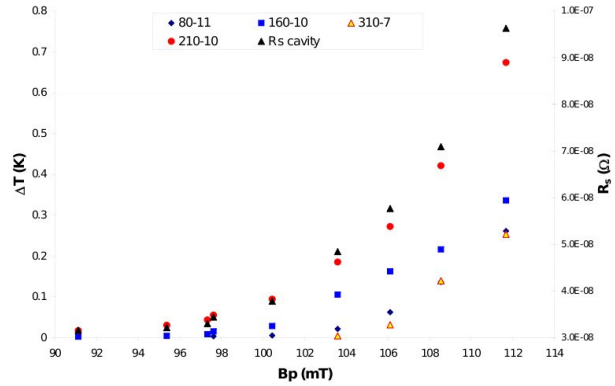

Figure 4: Experimental $R_s(2K,B)$ and $\Delta T(\mathbf{r},B)$ values of four hot spots of [5,15a] versus B.

PHENOMENOLOGY OF HIGH E FIELD RESULTS

In a first summary on HFQ in spun, i.e. heavily cold worked, rough Nb cavities produced by V.Palmier*i* and BCP stripped by P.Kneisel in [4,7a] and by M.Pekeler [14] it was shown for $7 \leq E_{acc}/MeV/m \leq 25MeV/m$ that HFQ is T independent and HFQ heat maps $\Delta T_{ou}(B,\mathbf{r})$ give crucial insights in Figs. 2 and [5,15]:

firstly, for rough, heavily cold worked ~100µm BCP stripped Nb sheath for $B_{pmax}<60mT$ hot spots are distri-buted uniformly on rings $E_{loc}=constant \leq E_p$ becoming larger hot spots for 230µm BCP stripped, spun surfaces, occurring at higher fields $B_{pmax}>60$ mT with $E^*_{loc} \sim E_P/5$ closer to the equator in Fig.2 [14]. Deep drawn, small grain Nb after 200µm BCP stripping show more homogenous surfaces with $B_{pmax} \sim 100$ mT for $E^*_{loc} \sim E_P/8$ with hot spots starting 2cm from the equator in [5,15].

secondly, hot spots show exponentially with E increa-sing $\Delta T_{ou}(\mathbf{r},E)$ following Eq.(4.2) with large spatial size $A^{**}_{ITE}(E)$ expanding with field toward the equator in contradiction to classical thermal diffusion

thirdly, UHV or air baking (>12h) between 100 and 160°C for about 12h reduces HFQ drastically still showing the exponential ITE dependencies. Large grain cavities show nearly no HFQ after UHV anneal [15c];

fourthly, removing 20 nm Nb after UHV anneal at 120°C by anodization restores HFQ properties [5];

fifthly, the exponential ITE field dependence governs the observed $\Delta T_{ou}(f\sim1\text{-}3GHz,B)$ dominating HFQ.

The detailed analysis of results shown in Figs.2-5 and Tables 1-2 and sketched in Sects.1-4 is to be found in [5] and can be summarized in short: The HFQ limitation at $Q_0 \sim 10^8 - 10^9$ is given by the HFQ source and valve terms, i.e. by the number of hot ITE broken pairs being BCS amplified. This number increases exponentially with $ß_{ave}/\varepsilon_r(d,n_L)$ and linearly with n_L and with spots like oxidized dislocations where broken pairs sneak into $|\varepsilon| \geq \Delta_{ave}$ regions existing in large numbers by wet oxidation. By ~120°C UHV annealing or dry oxidation n_L. and, e.g. oxidized dislocations, are reduced but precipitation grow and ITE broken pairs are confined in $|\varepsilon| \leq \Delta_{ave}$ wells reducing HFQ.

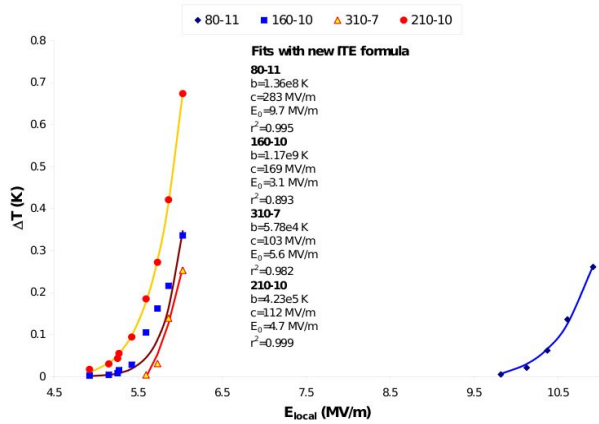

Figure 5: $\Delta T(\mathbf{r},B)$ fit Eq.(4.2) excellently with E_{loc} of the spot yielding

Table 2: After initial cleaning of a CEBAF Nb cavity built of bulk, small grained (~50µm), RRR > 300 Nb, 130µm have been stripped by BCP followed by 120°C baking for 48h at atmospheric pressure in flowing, hot N_2 by which Δ/kT_c increased from 1.7 to 1.86 [15a,b]. The position of dominating hot spots is about at 2cm distance to the equator with $E_p/8$. Fit parameters to $R_s(2K,B)$ after flowing N_2 (air) baking show drastic changes for the amplitude b, only.[5]

	R_{res}/nΩ	R_{res}^1/nΩ	γ^*	b/µΩ	c/MVm	E^0/MV/m
BCP	1.1	$3\cdot10^{-3}$	1.96	$2\cdot10^3$	990	3.0
120°C 48h	11	4·10-5	2.86	3.4·108	1277	8

CONCLUSIONS

The greatest achievement of our HFQ theory is the quantification of global and local exponential increases of $R^E(E)$ and $\Delta T_{ou}(E)$. After various surface and heat treatments at various labs ITE fits with one constant b and minimal error bars $r^2>0.99$, shown e.g. in Tables 1–2, Figs.2-5 and in [5,15] have been found. The obtained c- and E_0- ITE fields agree quantitatively with intrinsic tunnel properties of Nb_2O_5 and the HFQ amplitude b changes with treatment are explained in [5] by properties of the metallic NbO_x/Nb interface defining HFQ source and valve term and BCS amplification defining the HFQ loss term. The excellent consistency in different runs and

the small differences between c and E^0 in $R^E(E)$- and $\Delta T_{ou}(E)$- fits confirm that the BCS amplification by $\Delta T^*_{in}(E)$ adds no large E dependencies, i.e. $\Delta T^*_{in}(E) \sim R^E(E) \sim \Delta T_{ou}(E)$ holds. Essential in identification and in clarifying HFQ have been the detailed measurement and analysis of hot spot temperatures $\Delta T_{ou}(E,\mathbf{r})$ increasing exponentially with E, as $R^E(E)$ does. Because HFQ, e.g. in Figs. 2– 5 [14,15], is dominated by ballistic heat transfer yielding extended hot spots with stable rf operation down to $Q_0 \sim 10^8$ -10^9 [2,7,14,15] without thermal run away in contrast to cases of bad spots heating locally caused, e.g. by $R^{WL}{}_{res}$ and $R^{WL}{}_{hys}$. the size and distribution of HFQ hot spots changes strongly from rough, heavily cold worked to single crystal Nb cavities, e.g. Fig. 2 or [5], and rule out bad spots of both, dielectric $\sim R^E E^2$ or magnetic shielding current $\sim R^B B^2$ type. But the above elaborated combined action of the HFQ source term of the dielectric, the HFQ valve term of the metallic part of the interface and the BCS amplification loading the Q_0 down to about $Q_0 \sim 10^9$ can explain all observations, e.g. the effect of baking or anodizing – see [5]. The shift and growth $A_{ITE}{}^{**}$ of dominant hot spots towards the equator to fields above B_{Pmax}>160mT with BCP stripping homogenizing Nb surfaces and the strengths of baking effects are hints to specific $Nb_2O_5/NbO_x/Nb$ interface effects which can be reduced further only by proper understanding of the interface physics [5,11]. Because this interface physics is based on the p-d bonding in Nb_2O_5 and its volume increase an interface layer with high Nb^{4+}- and O- densities and therewith higher $n_L(z)$ seem unavoidable.

One obvious proposal are Al over layers on top of clean Nb avoiding not only crack corrosion as, e.g. NbN overlayers do [8], but Al_2O_3 shows also a factor 100 smaller n_L density reducing ITE correspondingly [6] as found

In comparing HFQs with the exponentially increasing field emission the FE source term $\sim \exp(c_{FEM}/ß_{FEM}E)$ corresponds to ITE broken pairs as HFQ source. The impact of accelerated electrons onto Nb cavity walls relax into hot quasiparticles showing up in traces perpendicular to the equator which initiate BCS amplification being so similar to the HFQ loss term

ACKNOWLEDGEMENT

Thanks go to Michael Pekeler and Gigi Ciovati for careful measurements and analysis.

REFERENCES

[1] Proc. First -, Second -,…. Ninth- workshop on rf Supercond. (Karlsruhe, 1980; CERN, 1984; ANL, 1987 … LASL, 1999).
[2a] J. Halbritter, J. Appl. Phys. 41, 4581 (1970), P. Kneisel et al., J. Appl. Phys. 44, 1785 (1973).
[2b] J. Halbritter, Z. Phys. 266, 209 (1974), J. P. Turneaure et al., J. Supercond. 4, 341 (1991).
[3] J. Halbritter, Z. Phys. B31, 19 (1978).
[4] J. Halbritter et al., IEEE Trans. Appl. Super. 11, 1864 (2001).
[5] J. Halbritter, to be submitted to PRST-AB.
[6a] J. Halbritter, Proc. 2. worskhop on Rf superconductivity Geneva, 1984 (CERN report,1984).
[6b] M. Regier et al., IEEE Trans. Appl. Super. 9, 2375 (1999).
[7a] J. Halbritter, Proc. 38 Eloisatron Workshop, Erice, Oct. 1999 (World Science Publ., Hongkong, 2000), p. 59.
[7b] J. Halbritter, SRF 2001 (KEK-Proc. 2003-2), p. 292
[7c] J. Halbritter, J. Appl. Phys. 97, 083904 (2005).
[8] J. Halbritter, Appl. Phys. A43, 1 (1987) and J. Less Common Metal. 139, 133 (1988) and ref. therein.
[9a] W. Schwarz, PhD thesis (Physics, Uni Karlsruhe, 1981) and J. Halbritter, Surf. Sci. 159, 509 (1985).
[9b] J. Halbritter, J. Appl. Phys. 58, 1320 (1985).
[10a] M. Grundner and J. Halbritter, Surf. Sci. 136, 144 (1984).
[10b] M. Grundner and J. Halbritter, J. Appl. Phys. 51, 397.
[11a] M. Delheusy et al., Appl. Phys. Lett. 92, 101911 (2008) and PhD thesis, Max Planck institute Stuttgart (2008).
[11b] O. Romanenko, PhD thesis (Cornell University, 2009) and Proc. SRF09 workshop TUOAAU02 (Berlin, 2009).
[11c] B. Visentin et al, ibid TUPPO047 (Berlin, 2009).
[12a] A. DasGupta et al., J. Appl. Phys. 47, 2146 (1976).
[12b] J. Mondal et al., Proc. SRF09 workshop THOAAU01 (Berlin, 2009).
[13] Ily-Jiun Chang and D. J. Scalapino, J. Low Temp. Phys. 31, 1(1978).
[14] M. Pekeler, PhD thesis (Uni Hamburg, 1996).
[15a] G. Ciovati, PhD thesis (Old Dominion University, Norfolk, 2005) and private communication.
[15b] G. Ciovati, J. Appl. Phys. 96, 1591 (2004).